Temperature-Entropy Wave in Self-Organized ^{4}He

Departmental Honors Thesis

Wayne M. Schlingman
The University of New Mexico
Department of Physics and Astronomy

Monday April 26th, 2004

1 Abstract

We[†] report a new experimental method for determining the velocity of the temperature-entropy wave that propagates through ^{4}He on its self-organized state. Over 50 datasets were examined in order to locate two that provide information on the velocity of this recently discovered mode. This velocity is expected to increase as Q^3, where Q is the heat flux that creates the self-organized critical state. We developed three different coding algorithms for data analysis and our results agree with earlier data that were obtained using a time-of-flight pulsed technique. From the information that we gathered by looking at the data, new data will be collected that specifically isolates the information we are looking for.

[†]Work done in collaboration with D. Sergatskov, S.T.P. Boyd, Q. Li, and R.V. Duncan at The University of New Mexico.

Contents

List of Figures

2 Introduction and Theory

2.1 Helium at Low Temperatures

Helium was first observed in 1868 by an astronomer looking at the elements in the sun, by finding absorption lines that did not match any known element. This element was given the name helium, after the word *Helios*, the sun. It was later discovered on Earth in 1895. Since then people have experimented on helium to test fundamental theories in physics, because complexity associated with chemical bond dynamics is nearly absent since helium is nearly chemically inert. Helium was first liquefied in 1908 by Heike Kamerlingh Onnes. Soon after, attempts were made to solidify helium, but it would not solidify under its own vapor pressure. Onnes also discovered that helium reached a maximum density at $2.2K$, and when they went to cooler temperatures the helium would suddenly stop boiling[1].

In 1923, the specific and latent heats were measured near $2.2K$ with signs of a discontinuity. In 1927, this point was identified as the transition temperature between two phases of helium, He-I (normal fluid) above the transition and He-II (superfluid) below. The year 1940 brought about new advances for the theoretical side of understanding helium at low temperatures. Laszlo Tisza was the first to explain the nature of the superfluid phase using a two-fluid model. Lev Landau improved this model in the following years and developed the Landau two-fluid model. The model refers to He-II as a mixture of two fluids. This superfluid component represents the part of the ^{4}He sample that occupies the lowest attainable quantum state of the system, and hence it is a "Bose-Einstein Condensate" of the interacting system of the ^{4}He atoms. This superfluid possess no entropy and hence is at absolute zero temperature. In the model the two fluids are completely mixed and non-interacting. The total density of He-II is then the sum of the superfluid fraction and the normal fluid fraction. Above the transition temperature the superfluid fraction is zero, while below the transition this superfluid fraction increases with decreasing temperature, reaching 100% only at absolute

[1] William Moeur's Ph.D. Thesis, UNM. 1997

zero[1]. Heat transport is then described by a two-fluid convective process with no net fluid flow, where the superfluid and normal fluid move in opposite directions to make the net fluid flow zero, while only the entropic normal fluid transports heat energy. The superfluid flows along any gradient in T, while the normal fluid travels against the gradient. Again, only the normal fluid transports heat.

The phase transition for ^{4}He is unique in that helium is the only material that does not turn into a solid at sufficiently low temperatures under its own vapor pressure. It instead has a phase transition to the superfluid He-II state. The phase diagram for ^{4}He is shown in Fig. 1. The transition between normal and superfluid helium occurs long the lambda line, and each point on the lambda line is the static superfluid transition temperature $T_\lambda(P)$, where P is pressure. This transition line has a negative slope as displayed in Fig. 1. The slope, $\frac{dT_\lambda}{dP}$, is negative, causing the gradient in T_λ to point in the opposite direction of gravity. The transition line is curved, but due to the small pressure variation over the $1cm$ tall cell, it can be assumed to be locally linear near saturated vapor pressure(SVP) where the He-II, He-I, and vapor phases meet. In one dimension, $\vec{\nabla}T_\lambda = \frac{dT_\lambda}{dz} = \rho g \frac{dT_\lambda}{dP}$ where ρ is the liquid ^{4}He density(at $T = T_\lambda(SVP)$, $\rho \cong 0.147 \frac{g}{cm^3}$), and $\vec{g}$ is the gravitational acceleration($g = 9.8 \frac{m}{s}$).

2.2 The Cell and Helium System

The experiments were performed on a cryostat that contains several stages of thermal control. The experimental cell that contains the helium resides on the bottom stage of the cryostat where the thermal isolation is adequate to permit temperature control near $2.2K$ to within a fraction of a nanokelvin. The cell itself is a small metal cylinder that is $2.4cm$ in diameter and about $1cm$ tall. The cell is capped by two metal end-plates that serve also as heat sinks and sources. Both plates have heaters thermally connected to them. The top plate heater provides a steady heat flux through the cell, and the bottom heater is used to provide time varying heat that is used to measure the thermal properties described below.

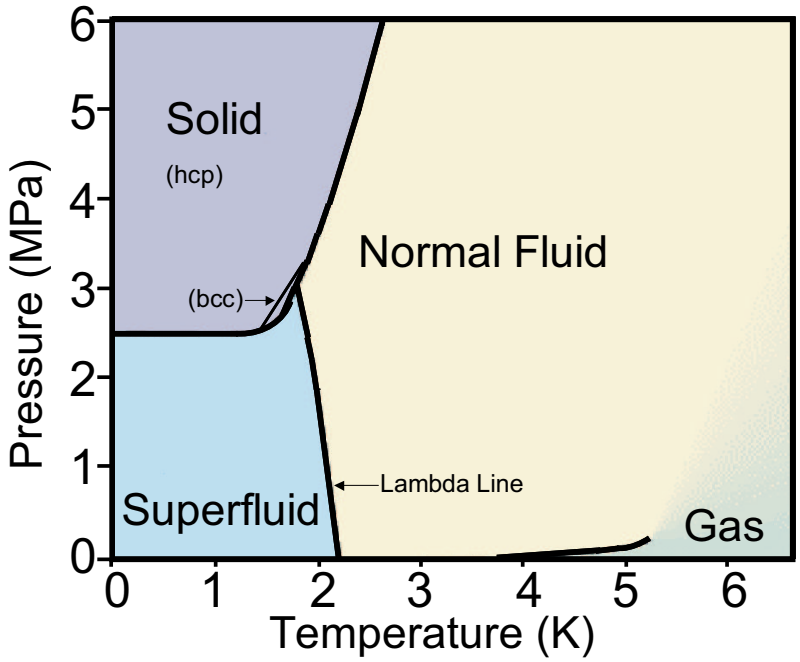

Figure 1: The Phase Diagram for ^{4}He: Ref. [9]

The steady heat flux flows from the top of the cell to the bottom of the cell, called the heat-from-above (HfA) configuration. The heater on the top plate puts the heat into the cell and the bottom plate is linked to a cooling stage that pulls the heat out at the same rate when the cell reaches steady state. This cooling stage, which is maintained at its operating temperature below T_λ to within a noise level of about 1 nanokelvin, is connected to the cell bottom through a thermal resistance of 2,000 $\frac{K}{W}$, which is much larger than any internal thermal resistance in the cell (See Fig. 2). This causes the cell to be held in a state of constant heat flux, so the cell is current biased, and no stage temperature is directly controlled on the cell. This means the cell stage temperatures are free to self-adjust in any manner in response to additional added heat, as long as the applied steady heat flux, Q, is maintained.

2.3 The Cell

The cell is designed to be azimuthally and radially symmetric, so it can be considered a 1-dimensional entity with temperature variations only along its height. Of course there

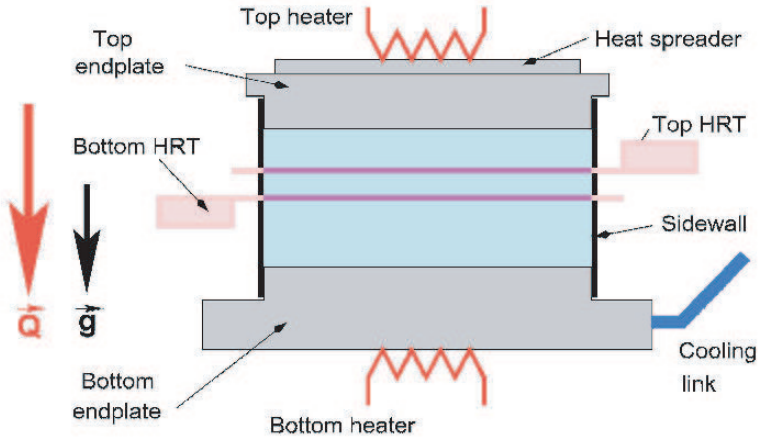

Figure 2: A Schematic Diagram of the Cell

are radial and azimuthal variations in the cell as well, but they are very small and below the noise level, so they can be ignored. To measure the heat transport states in the helium we need devices that can measure temperature to a very high precision at various positions along the cell height. The two thermometers that are used to measure the helium temperatures are located on the sidewalls of the cell with a spacing of $2.4mm$ between each other. The cell sidewall consists of $75\mu m$ thick stainless steel, with two $125\mu m$ thick copper foils penetrating the sidewall to provide a low thermal resistance path between the thermometer that attaches to the foil and the helium at the probe's position along the height of the cell. These thermometers are called High Resolution Thermometers(HRTs).

2.4 High Resolution Thermometers

HRTs consist of the paramagnetic material Palladium Manganese[2], PdMn, machined into a cylinder and wrapped in a superconducting coil, and placed in a superconducting "flux

[2]B.J. Klemme, M.J. Adriaans, P.K. Day, D.A. Sergatskov, T.L. Aselage, R.V. Duncan, J. Low Temp. Phys. **116** (1999).

tube" that traps a constant magnetic field on the PdMn. The superconducting coil that is wrapped around the PdMn cylinder is connected to a Superconducting Quantum Interference Device(SQUID) so that any change in magnetic flux threading the PdMn is detected by the SQUID. The paramagnetic material, PdMn, is maintained just above its Currie temperature where it has a strong temperature dependent magnetic susceptibility. When PdMn is placed in a constant magnetic field, it develops a magnetization that is proportional to its susceptibility. Therefore, as the temperature changes the magnetic susceptibility changes and so does the magnetization of the PdMn pill. The superconducting circuit detects this change in magnetization using the SQUID. This flux change within the SQUID is calibrated against the temperature change of the PdMn that induced it. Temperature changes as small as $0.1nK$ in a one Hertz measurement bandwidth may be detected in this manner, and the demonstrated drift of these devices is $< 10^{-14}\frac{K}{s}$.

When beginning an experimental run, the cell is first cooled down into the^{4}He superfluid state. With the cell entirely superfluid and hence with infinite thermal conductivity, we apply a heat flux, $\vec{Q}$, through the cell, and adjust the cooling stage temperature until steady state is reached. Once this occurs, the heat flux is increased by a small amount, causing He-II to slowly warm up until the cell reaches the critical temperature, T_c, where the SOC state forms. The SOC state forms at the bottom of the cell and moves upward as more heat is supplied to the cell. As explained in section 2.6, T_c is dependent on the heat flux put through the sample of He-II[3].

$$T_c(Q) = T_\lambda - T_\lambda \left(\frac{Q}{Q_o}\right)^y,\ y = .813 \pm .012,\ Q_o = 568 \pm 200\frac{W}{cm^2},\ T_\lambda = 2.1768K$$

Higher values of heat flux, $Q = |\vec{Q}|$, depress the critical temperature farther below T_λ, where T_λ is the static superfluid transition temperature. T_c decreases with Q,[3] and in the limit that Q goes to zero T_c reaches its maximum value at T_λ. This depression of T_c with Q is similar

[3]R.V. Duncan, G. Ahlers, and V. Steinberg Phys. Rev. Lett. 60, 1522 (1988).

to the depression of the superconducting transition temperature in a wire as its electrical current is increased.

2.5 Existence of the Self-Organized Critical State

When a heat flux Q flows from the top to bottom in a liquid helium cell that is close to its superfluid transition temperature, such as the cell in Fig. 2, the helium in the cell can self-organize such that the resulting temperature gradient, $\vec{\nabla}T$, equals the gradient across the cell of its superfluid transition temperature, $\vec{\nabla}T_\lambda$, which, as discussed above, is due to the pressure gradient across the sample, is a constant $1.273\frac{\mu K}{cm}$ and $\vec{\nabla}T_\lambda$ points in the opposite direction to $\vec{g}$, where $\vec{g}$ is the acceleration due to Earth's gravity. This has been observed to occur as $\vec{Q}$ is varied over three orders of magnitude, as described in Moeur *et. al*[4]. This is amazing, in that the thermal gradient across the cell remains at a constant $1.273\mu K/cm$ as $\vec{Q}$ is changed by over a factor of one thousand! While this self-organization seems remarkable, it results naturally from the divergence in the thermal conductivity of ^{4}He at T_c, where T_c is the temperature where the superfluid's perfect thermal conductivity fails catastrophically as discussed above. This divergence in the ^{4}He thermal conductivity has been observed in many other experiments[5] and has been understood using dynamic scaling theory[6]. The microscopic nature of this SOC state for $Q > 200\frac{nW}{cm^2}$, where $T_{soc}(Q) < T_\lambda$, is unclear and is the subject of current research[7], $T_{soc}(Q)$ is the temperature at which the cell fully self-organizes at a given Q.

But why does the liquid helium's thermal conductivity diverge as $T_c(Q)$ is approached from above(by cooling the cell)? Since the superfluid transition is a continuous or "second order" phase transition, fluctuations of the ordered phase in the disordered phase become large

[4]W. A. Moeur, P. K. Day, F-C. Liu, S. T. P. Boyd, M. J. Adriaans, R. V. Duncan Phys. Rev. Lett. 78, 2421 (1997).

[5]W.Y. Tam and G. Ahlers, Phys. Rev B **32**, 5932 (1985; **33**, 183 (1986). and M. Dingus, F. Zhong, and H. Meyer, J. Low Temp. Phys. **65**, 185 (1986).

[6]R.A. Ferrell, N. Menyhard, H. Schmidt, F. Schwabl, P. Szepfalusy, Phys. Rev. Lett. 18 (1967) 891.

[7]P.B. Weichman, J. Miller, J. Low Temp. Phys. **119** (2000).

as the critical temperature, T_c, is approached from above. The "ordered phase" is the superfluid phase which has infinite thermal conductivity, so the otherwise highly thermally resistive helium is effectively shorted out by these fluctuations into the superfluid phase. Hence the observed total thermal conductivity κ(defined as the reciprocal of the thermal resistivity) ρ, of the normal fluid ^{4}He very close to its critical point diverges as $\kappa(\epsilon) = \kappa_\circ \epsilon^{-x}$ where $x \cong \frac{1}{2}$, $\kappa_\circ \simeq 10^{-5} \frac{W}{cm\,K}$, and $\epsilon \equiv \frac{T - T_c(Q)}{T_\lambda}$ is the measure of the distance of the ^{4}He from its critical point. Since the pressure dependence of $T_c(Q)$ is the same as that of T_λ, $\nabla T_c(Q) = \nabla T_\lambda = 1.273 \frac{\mu K}{cm}$ at all Q. This self-organized state is easily predicted theoretically by numerically integrating the static heat flow equation, $-\kappa \vec{\nabla} T = \vec{Q}$, to obtain the thermal profile across the cell with the singular κ at T_c, with the boundary conditions that Q enters the top of the cell and is extracted from the bottom[8].

Here is a theoretical treatment that describes the time-independent SOC state. Let the z-axis be along the cell axis pointing up, opposing gravity. In one-dimension the heat transfer equation $\vec{Q} = -\kappa \vec{\nabla} T$ becomes:

$$Q = \kappa \frac{\partial T}{\partial z} \tag{1}$$

We know that on the SOC state

$$\frac{\partial T}{\partial z} = \frac{\partial T_\lambda}{\partial z} \equiv \alpha = 1.273 \mu K/cm \tag{2}$$

Hence,

$$\frac{\partial T_\lambda}{\partial z} = \frac{Q}{\kappa} \tag{3}$$

so κ must increase in proportion to Q to keep $\frac{dT}{dz} = \frac{dT_\lambda}{dz} = constant$. The thermal conductivity of the SOC helium is described by

$$\kappa = \kappa_\circ \epsilon^{-x} \tag{4}$$

[8]William Moeur's Ph.D Thesis UNM 1997

Where ϵ is the reduced temperature, with $\kappa_o \approx 10^{-5}\frac{W}{cmK}$, $x \approx .48$ both of which have been determined experimentally by Moeur *et. al*[9]. Taking into consideration that we only have one direction $\vec{z}$ we only have to deal with magnitudes. The ^{4}He thermal conductivity is defined as

$$\kappa = \frac{Q}{\nabla T} \tag{5}$$

And thus on the SOC state, where $\nabla T = \nabla T_\lambda$, the thermal conductivity becomes:

$$\kappa_{soc} = \frac{Q}{\nabla T_\lambda} \tag{6}$$

Combining this and the power law dependence of κ on ϵ (eq. 4), the reduced temperature on the SOC state is::

$$\epsilon_{soc}^{-x} = \frac{Q}{\nabla T_\lambda \cdot \kappa_o} \tag{7}$$

Hence the self organization temperature $T_{soc}(Q)$ is:

$$\frac{T_{soc} - T_c}{T_c} = \left(\frac{Q}{\kappa_o \cdot \nabla T_\lambda}\right)^{\frac{-1}{x}} \tag{8}$$

Therefore each value of Q will correspond to a specific $T_{soc}(Q)$ value that permits the thermal conductivity κ to achieve κ_{soc} so that the cell can self-organize with $\nabla T = \nabla T_\lambda$.

2.6 New Propagating Mode

Recently a new temperature-entropy wave has been observed experimentally[10] to propagate only against the vector direction of $\vec{Q}$ on this new SOC state. This mode is easily understood by integrating the full time dependent heat flow equation, as described below. The temperature-entropy wave will only propagate along the SOC state when heat pulses are

[9]W. A. Moeur, P. K. Day, F-C. Liu, S. T. P. Boyd, M. J. Adriaans, R. V. Duncan Phys. Rev. Lett. 78, 2421 (1997).

[10]D. A. Sergatskov, A. V. Babkin, R. A. M. Lee, S. T. P. Boyd, R. V. Duncan Physica B. 329-333, 208 (2003).

applied to the bottom plate in the HfA configuration[10]. This wave propagates only against the heat current $\vec{Q}$, hence from the bottom to the top of the cell. The time-dependent heat diffusion equation is obtained by combining the heat energy continuity equation with Fourier's Law:

$$C_{soc}\frac{\partial T}{\partial t} = -\vec{\nabla}\cdot\vec{Q},\ \vec{Q} = -\kappa\vec{\nabla}T \tag{9}$$

Where C_{soc} is the heat capacity on the SOC state. Here κ depends on z since κ depends on T, and hence varies across the cell due to the thermal gradient. In one-dimension:

$$C_{soc}\frac{\partial T}{\partial t} = \kappa\frac{\partial^2 T}{\partial z^2} + \left(\frac{\partial \kappa}{\partial z}\right)\left(\frac{\partial T}{\partial z}\right) \tag{10}$$

The first term on the RHS is the conventional result when κ is just a function of position, and the second term on the RHS results from the gradient of κ. If we convert the equation to reduced temperature, $\epsilon = \frac{T-T_c(Q)}{T_\lambda}$, and assume small heat pulses, $\frac{\partial \epsilon}{\partial z} \ll \frac{\alpha}{T_\lambda}$, eq. 10 becomes:

$$C_{soc}(\epsilon)\frac{\partial \epsilon}{\partial t} = \kappa(\epsilon)\frac{\partial^2 \epsilon}{\partial z^2} + \alpha\left(\frac{\partial \kappa}{\partial \epsilon}\right)\left(\frac{\partial \epsilon}{\partial z}\right) \tag{11}$$

Where $\alpha \equiv \frac{dT_\lambda}{dz}$, $\frac{d\epsilon}{dz} = \frac{1}{T_\lambda}\left(\frac{dT}{dz} - \nabla T_\lambda\right)$. Recall that T_λ and T_c have the same gradient $= 1.273\frac{\mu K}{cm}$. Also, $\frac{d\epsilon}{dt} = \frac{1}{T_\lambda}\frac{dT}{dt}$. Since $\kappa = \kappa_o\epsilon^{-x}$, $\frac{\partial \kappa}{\partial \epsilon} = \frac{-x\cdot\kappa(\epsilon)}{\epsilon}$ and eq. 11 becomes:

$$C_{soc}(\epsilon)\frac{\partial \epsilon}{\partial t} = \kappa(\epsilon)\frac{\partial^2 \epsilon}{\partial z^2} - \frac{\alpha x}{T_\lambda}\frac{\kappa(\epsilon)}{\epsilon}\frac{\partial \epsilon}{\partial z} \tag{12}$$

Now, let $\epsilon(z,t) = \epsilon_{soc} + \delta(z,t)$, where $\delta(z,t)$ is composed of damped, Fourier components:

$$\delta(z,t) = \int \delta(k)e^{-Dk^2t}e^{ik\cdot(z\pm ut)}dk \tag{13}$$

Note that ϵ_{soc} is the steady state solution that is independent of space and time. The $(+)$ selection in $z \pm ut$ corresponds to motion in the $-z$ direction (along Q) and the $(-)$ corresponds to motion in the $+z$ direction (against Q). D is the damping coefficient. Substitute

eq. 13 into eq. 12, and in the linear limit $\delta(z,t) \ll \epsilon_{soc}$:

$$C_{soc}(\epsilon_{soc})(-Dk^2 \pm iku) = \kappa_{soc}(ik)^2 - (ik)\left(\frac{\alpha x \kappa_{soc}}{\epsilon_{soc}}\right) \tag{14}$$

Solve for the real and imaginary components individually. From the imaginary component we get

$$D = \frac{\kappa_{soc}}{C_{soc}} = \frac{Q}{\alpha C_{soc}} \propto Q \tag{15}$$

assuming C_{soc} is not dependent on Q. If D varies linearly with Q then this will confirm that C_{soc} is independent of Q. For the real part of eq. 14 the negative sign is the only non-trivial solution, thus the wave only propagates only against the heat flow and with a velocity u, where

$$u = \frac{\alpha x \kappa_{soc}}{T_\lambda C_{soc}} = \frac{xQ}{C_{soc}T_\lambda} \cdot \left(\frac{Q}{\kappa_o \alpha}\right)^{\frac{1}{x}} \propto Q^{3.1} \tag{16}$$

This is the physical origin of the new SOC state temperature-entropy wave[11].

3 The Self-Organized Critical State

Self-organized criticality occurs in many systems in Nature. In its most general form, self-organization occurs when a system is driven away from equilibrium and self-adjusts to its critical line[12], where some generalized susceptibility diverges. In our case this critical line is the lambda line in Fig. 1, and the generalized susceptibility is the thermal conductivity κ. In this case the system is driven away from equilibrium by the heat flux Q.

[11] D. A. Sergatskov, A. V. Babkin, R. A. M. Lee, S. T. P. Boyd, R. V. Duncan Physica B. 329-333, 208 (2003).

[12] *How Nature Works*, Per Bak

3.1 An Upper Heat Flux?

As discussed above,

$$\kappa_{soc} = \frac{|\vec{Q}|}{|\vec{\nabla} T_\lambda|}, \quad \nabla T = \nabla T_\lambda = \frac{Q}{\kappa(\epsilon_{soc})}$$

Thus the conductivity of SOC helium must vary linearly with the magnitude of heat flux passing through the cell. For larger values of Q, the superfluid helium (which has infinite thermal conductivity only in the $Q = 0$ limit) begins to form a thermal gradient as well, with $\nabla T_{II} \sim Q^3$ where ∇T_{II} is the superfluid temperature gradient that results from "mutual friction" between the normal fluid and superfluid components as high counter flow velocities. Define the superfluid thermal resistance

$$R_{II} = \frac{\nabla T_{II}}{Q}$$

and the associated ^{4}He-II conductivity:

$$\kappa_{II} \propto \frac{1}{R_{II}}$$

Since $\nabla T_{II} \propto Q^3$, eventually $\nabla T_{II} > \nabla T_\lambda$ as Q is increased. Define Q_c as the heat flux where $\nabla T_{II}(Q = Q_c) = \nabla T_\lambda$. Experimentally when Q exceeds Q_c ($Q_c \approx 30 \mu W/cm^2$)[13] the SOC state may collapse. The nature of the self-organized critical state will be explored for values of Q near and above Q_c in an upcoming experiment, which is being taken cold now.

4 The Project

The bottom heater imparts a small sinusoidal heat flux through the cell that travels in the opposite direction of $\vec{Q}$. This time varying flux is only a small perturbation to the dynamics of the cell helium, so its non-linear effects are ignored as explained above. When looking at

[13] D. A. Sergatskov, A. V. Babkin, R. A. M. Lee, S. T. P. Boyd, R. V. Duncan Physica B. 329-333, 208 (2003).

the data, we know that the temperature-entropy wave will hit the bottom thermometer first as it propagates against the direction of $\vec{Q}$. When this happens the bottom thermometer registers the sinusoidally varying temperature disturbance. As the wave travels through the helium another $2.4mm$, a certain time passes and hence the phase of the wave changes at the upper probe. It takes a specific amount of time, Δt for the wavefront to travel between the probes, which is simply $\Delta t = \frac{2.4mm}{v_{soc}(Q)}$, where $v_{soc}(Q)$ is the velocity of the wave through the helium. Hence, we can infer a velocity based on the phase shift, $\Delta\phi = \frac{2\pi\Delta t}{\tau}$ where tau is the period of the applied oscillation, of the temperature-entropy wave between the measurements made on the bottom and top HRTs. So the majority of the project involved looking at data sets and attempting to determine the phase shifts between the top and bottom thermometers. We tried this in many different ways, but only one algorithm seemed to do the job well. All three methods will be discussed in the following subsections. We did get one good data point giving a velocity of $10.1 \pm .3\frac{mm}{sec}$ at $Q = 100\frac{nW}{cm^2}$, which appears to fit with the previously measured data, as discussed below.

4.1 Fourier Transform

The first technique that we tried was a rudimentary Fourier Transform of the data. Let $s(t)$ be the data, then $x(\omega) = \frac{1}{T}\int_0^T s(t)cos(\omega t)dt$, whence ω is the frequency of the drive. Similarly, $y(\omega) = \frac{1}{T}\int_0^T s(t)sin(\omega t)dt$. Care was taken to make sure that T was an integral number of periods of the drive. We then integrated over the entire data set on the SOC state keeping track of the cumulative integral. By taking the arctangent of $\frac{y}{x}$ at values of $n\tau$, where n is an integer and τ is the period, we determine the phase of the wave relative to a sinusoidal current drive. After doing this for both the temperatures measured at the top and bottom probes, we subtract these phases from the top and bottom to determine the phase shift. Absolute phase is irrelevant in this situation, since the phase shift at the bottom cell end plate is unknown. However, relative phase is critical, as it shows the time displacement of the wave as it passes by the two separate thermometers. With the time it takes for

the wave to pass both thermometers, the velocity is then determined using $v = \frac{2.4mm}{\Delta t}$ and $\Delta t = \tau \times \frac{\Delta\phi}{2\pi} = \frac{\Delta\phi}{\omega}$ as $\tau = \frac{2\pi}{\omega}$.

One would think this technique would be very effective, and it is when noise-free artificial data is used. But when actual noisy data is used, it performs poorly. It does not have very good temporal resolution, and the phase shifts on many of the data sets were too small to determine. With the phases being very small, tiny jitter developed a noisy set of phase-shift data. Even with a line of best fit, or other ways of sampling determined in this way, the phases were still hidden in the noise. After many weeks of manipulating and changing the code, this method was incredibly slow, a resource hog, and hence not a reliable method of data analysis.

4.2 Cross-Correlation

The next method of determining the phase was using an cross-correlation between the top and bottom temperature measurements. In this case, the average temperature value was subtracted off leaving the processed probe temperatures oscillating about zero. Then, the bottom set of measurements was shifted by a single interval in time,Δt against the other.

$$I(\Delta t) = \frac{1}{T}\int_0^T s_{top}(t)s_{bot}(t+\Delta t)dt \tag{17}$$

The total integral was taken for each set. The total value of the integral, $I(\Delta t)$ is then plotted against Δt to determine the maximum, where the corresponding Δt is the time delay we seek. This method ignored the fact that the time spacing between the individual temperature measurements is not perfectly uniform. It assumed that the variations would be small and if the same range of data was used each time the effects would be minimized.

This method works well at giving a good estimate to the phase shift. It shows a clear sinusoidal variation in total value of the integral with respect to phase shift. The problems

stem from the lack of resolution between the data points. In many cases, the peak value of the integral would occur only after only one step. The maximum step was badly influenced by noise, because the noise variations are large. This gave only a ridiculously rough estimate of the phase shift. It works well for determining the phase-shift at a very quick glance. There is no effective way to make this analysis technique more accurate for noisy data. On data sets with a much higher temporal resolution between points, this technique may become a handy way of determining phase shifts to an acceptable degree of accuracy.

4.3 Correlation With an External Sine Curve

This method is by far the most accurate and simple of all the methods attempted thus far. It combines some of the aspects of each technique described above. It still multiplies a sine function to each of the data/temperature series and then integrates over the entire set. The information is then plotted and the trend is clearly sinusoidal. The phase is varied over 2π, with the range 2π divided into however many pieces as needed to obtain the desired phase resolution. In our case, data set was divided into 20 different sections, and the phase resolution used on each section was $\frac{2\pi}{10{,}000}$. The phase is changed very slowly allowing for tight resolution in the final set of information. With 10,000 steps between 0 and 2π the phase can be determined accurately. The phase for the top and bottom waves are measured individually and then the difference between them is determined by simply subtracting these phases.

The data analysis shows an average measured speed of $10.1 \pm .3 \frac{mm}{sec}$. There is some error to this, but it is much smaller than what was obtained using the pulsed Time of Flight(TOF) technique[14]. The phase here does not depend on the input time spacings, since the phase delay steps may be made very small. It just multiplies the data by the sinusoid shifted by the phase delay, and plots this integral against the phase delay. This allowed us to clearly

[14]D. A. Sergatskov, A. V. Babkin, R. A. M. Lee, S. T. P. Boyd, R. V. Duncan Physica B. 329-333, 208 (2003).

tell what the phase was even on high noise, low signals, since the average over many periods effectively canceled the noise. This method gives high resolution over the entire region of possible phase shifts. Any resolution can be taken from ten to millions of steps between 0 and 2π. So any periodic data with a well-defined frequency(for us the known drive frequency) can be matched with an appropriate phase shift. This means noisy data can be used and a decent value of phase can be found. As always, noise still plays a factor but this technique is less sensitive to noise that the other methods.

4.4 Original Velocity Measurement Methods - Pulse Technique

The initial velocity measurements of this new propagation mode where made using the pulsed TOF method[14]. This method is setup in exactly the same as discussed above, except the bottom heater is not providing a continuously varying heat current forming the wave. Instead, a single pulse is used and the time that the peak passes each probe is measured. This is a simple way of determining the speed of propagation as a single pulse measured at two different times will have a clear time delay because the rising, falling, and peaks of the pulse will be displaced. The sinusoidally varying method allows for many more measurements to be made over a period of time allowing random errors to effectively average to zero over many periods of the drive. This reduces the amount of error in the measurements and allows for more information to be extracted from the data.

5 Results and Methods

5.1 Data Preparation

This section will detail the method used to extract the phase difference out of the data. It will also explain were the results came from and illustrate some of the difficulties that were encountered along the way. To give an overview of how each file had to be dealt with, examples of each stage will be provided. First, all systematic artifacts were removed

from the data set. This data,which was taken by the SQUID, was clipped because of the small dynamic range of the SQUID between resets. So the data must be recomposed into a continuous sinusoidal curve by extracting the reset jumps. The next part of the process is to remove any lines that record the same information that was recorded in the previous measurement. This resulted from a registering error when the data was digitized. After the data has been recomposed and cleaned[†], it must be inspected visually to determine if it is worth analyzing. The data in Fig. 3(a) is good, there are no major discontinuities near the SOC state and there is a well defined SOC state. The SOC state is where the temperature profile becomes horizontal. As explained in detail Moeur *et al.*, the data becomes horizontal when the temperature at the thermometers location along the cell height can no longer change with time. This occurs when the helium at that height has self-organized, since after that $\nabla T = \nabla T_\lambda$, and hence the temperature at that height can no longer change. To determine the velocity of the SOC wave we start by selecting a time where both the top and bottom thermometers are both measuring SOC helium. There is no temperature difference between the upper and lower thermometers on the superfluid state(time less than $2,000s$ in Fig. 3(a)), so the top and bottom data are offset by about $425nK$ in Fig. 3(a). The SOC state is what is interesting us, so the data is chopped to display only the SOC state. We also want to compare the two thermometers side be side, so a constant value of $\Delta z \times \frac{dT}{dz} = 0.24cm \times 1.273\frac{\mu K}{cm}$ must be subtracted from the SOC state data to bring the two temperatures to the same baseline as shown in Fig. 3(b).

We next need to determine if the SOC data has a phase shift that may be resolved. Hence we zoom in on the data that we just chopped. The result is shown in Fig. 4, where the random noise in the data is visible. Note that the peak-to-peak variation of the data in Fig. 4 is only about $2nK$, so the noise of the measurements is apparent. Using the Fourier technique is difficult, because the noise was amplified and caused problems when taking the

[†]We only had to do this for 5 sets, Q. Li cleaned and prepared the data for the majority of data sets. The code to prepare the data was written by Q. Li and S.T.P. Boyd.

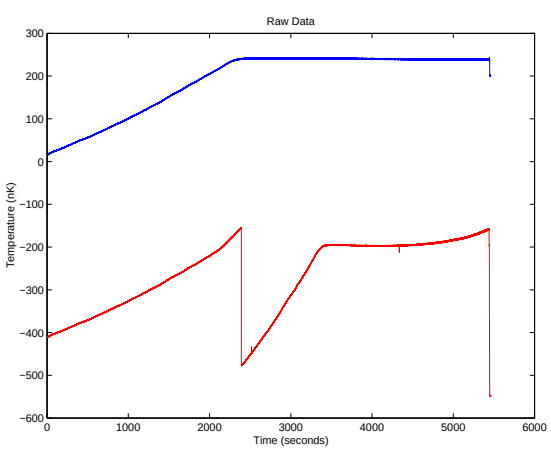

(a) A sample of data that has only been cleaned. The blue is the bottom temperature and the red is the top. The jump in the middle of the top (red) data is a SQUID jump.

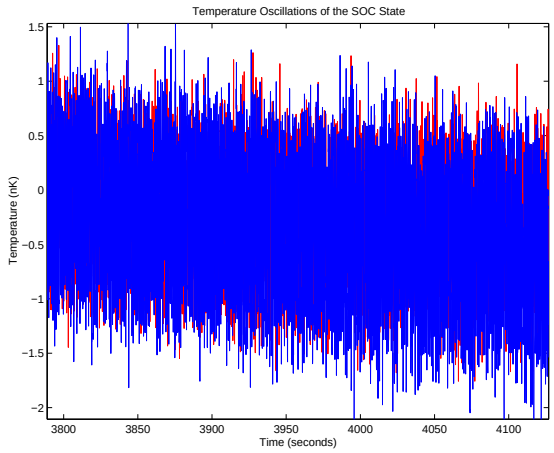

(b) A sample of data that has been subtracted and cut to include only the SOC state, and then plotter on a highly expanded scale.

Figure 3: Plots of the data as they appear throughout the analysis process.

arctangent, resulting in noisy phase information. The data can now be analyzed numerically knowing that there is a visible phase shift in the data that can be measured.

5.2 Locking Into the Data

This method was thought up after a long unsuccessful run at trying to get the other methods to provide reliable phase information. It is a combination between the a soft lock-in technique and the cross-correlation technique. It was built as a way around the problems previously faced, to allow the program to step through the phase shift, and then to see how valid that phase was. Beginning as a "guess and check method" it evolved into a self-sufficient algorithm that can pick the phase shift off any periodic sinusoid. Figures 5(a) & 5(b) show the sine curve as it passes over the data. Effectively, the phase of the sine curve is shifted until it best agrees with the periodic variation of the noisy data. It is like moving a puzzle piece into position, moving it until it fits into place. The code permits the user to define how many sections the SOC state is divided into, and how small a phase step to increment.

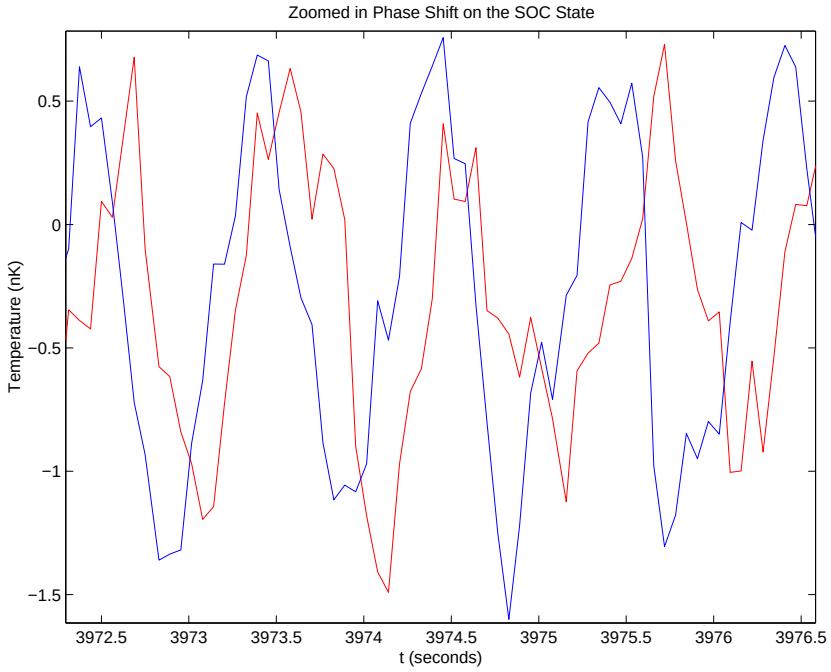

Figure 4: This is what the SOC state looks like after subtraction when we zoom in on it. The phase shift is easily seen between the two data sets. The blue represents the bottom thermometer, and the red the top.

This allows the resolution to be set by the user. In this analysis 10,000 units between zero and 2π was chosen to provide high resolution in a relatively short time. The next step is to numerically integrate, over the entire range of the SOC state, the data multiplied by a shifted sine curve, i.e. $data(t) \times sin(t + \phi)$. We change ϕ each time and record the value of integration at each phase shift ϕ.

5.3 Pulling Out the Phase

Now that we have numerically integrated over the entire range of data and possible ϕ values, the phase shift can be determined. By inspecting Fig. 6, the two curves represent the total values of the integrals for each phase shift. When the sine curve is in phase with the data, it gives the maximum value for the integral. When it is out of phase, it gives the lowest. So we compare the two maxima in Fig. 6 and compute the difference to get the phase delay. Where we find the maxima on the graph in Fig. 6 will give us fraction of 2π the phase is, with the absolute phase for each curve, with respect to an unshifted sine curve, given by

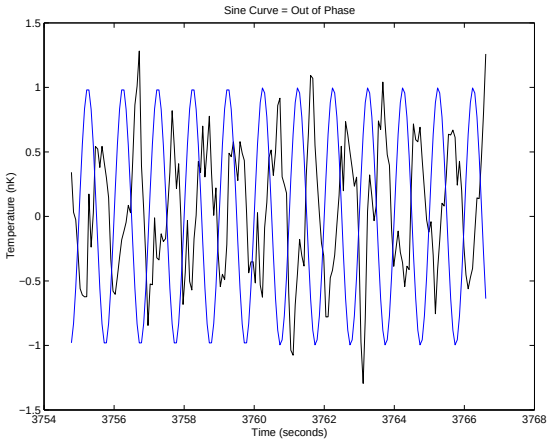

(a) A sample of when the sine curve is not in phase with the data.

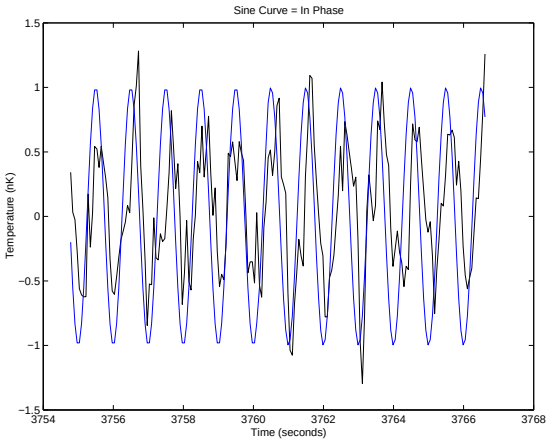

(b) A sample of when the sine curve is in phase with the data.

Figure 5: The sine curve is phase shifted until it best matches the period of the data.

$\phi_{1\ or\ 2} = 2\pi \times \frac{n}{10{,}000}$ where n is the number of steps the program has iterated through. With the "absolute" phase computed, we can determine the relative phase through subtraction. This gives two possibilities for a phase difference, $\Delta\phi = \phi_1 - \phi_2$ or $\Delta\phi = 2\pi - (\phi_1 - \phi_2)$. By inspection of the original SOC data in Fig. 4 one of the possibilities is incorrect, since the wave passes the lower thermometer first, leaving us with $\Delta\phi = \phi_1 - \phi_2$. When converted back to time units,$\Delta t = \frac{\Delta\phi}{\omega}$, we can determine the velocity of the wave knowing the spacing between the two thermometers is $d = 2.4mm$, where $v_{soc} = \frac{d}{\Delta t} = 2.4mm \times \frac{\omega}{\Delta\phi}$.

5.4 How Our Data Compares

After computing the phase shift and extrapolating the velocity from that, our measurement must be compared to those made previously through a pulse technique. The plot in Fig. 7 shows the previously taken data[15] as the red points and our data as the blue star in the upper right corner. Our velocity of $10.1 \pm .3\frac{mm}{sec}$ at a heat flux $Q = 100\frac{nW}{cm^2}$, fits right in line with those taken previously. Since our data was taken at a higher value if Q, we have extended the range in which the theory has been experimentally confirmed. We have another

[15]Data is from Sergatskov *et al.*

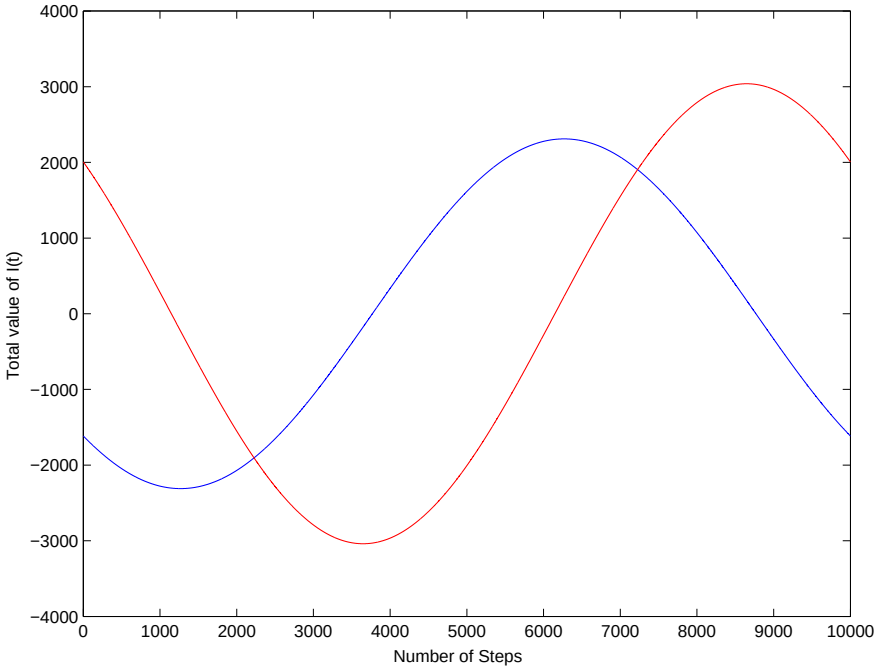

Figure 6: Here is the phase information after the sine curve has undergone a phase change of $n \times 2\pi 10^{-4}$ radians. The red curve corresponds to the bottom phase and the blue the top.

data point taken at very high levels of Q but we do not expect it to fit any range because it does not fit into the linear limit of our assumptions, $v = 36.5 \pm .2 \frac{mm}{sec}$. We also know that our analysis routines work because we extracted a valid phase. With minor modifications, the analysis tools we developed can be used on the other data sets to fill in the many points that are missing from this plot. This will be done this coming summer.

6 Discussion

We originally set out to compute phases for any file that came along, but after many trials and setbacks a change of focus was in order. This is when we came up with the idea of looking for files with distinct readable phase shifts and working from there. After this was done, we ended up with a single file that was useful to development of the code and beneficial to the science involved. The other files do contain important information regarding other physical measurements and will be studied, but at the time they did not meet the classification of being useful for developing an algorithm that was effective at determining the phase. The

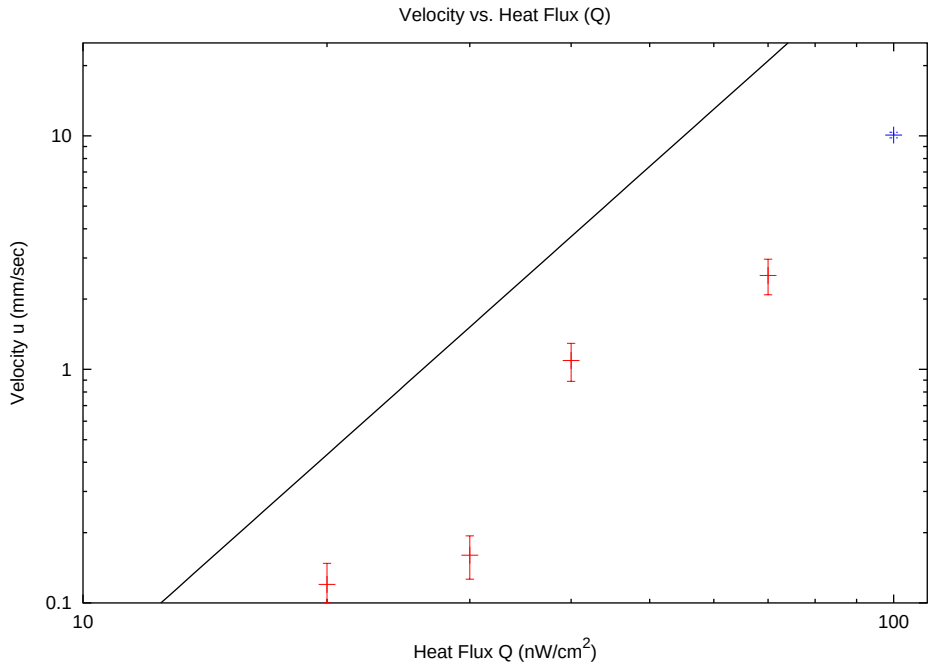

Figure 7: Here is the velocity data known for ^{4}He, $v_{soc} \sim Q^3$. The red points are from Sergatskov *et al.* and the blue point our new data point. The line corresponds to the Q^3 trend these points have, it is shifted by an arbitrary amount.

process was slow for much of the semester as the Fourier technique was very time consuming to write, modify, plan, and process. Not being incredibly versed in numerical methods, the planning it took to get the process and mathematics into the computer to a while. It took time to develop the code so it was robust enough to accept data instead of clean sample data. In the end, it did not produce what we needed it to. Since it was complicated, the idea was scrapped in favor of the more promising cross-correlation. This did not take as much time to write, but finding the phase information took hours of testing and tweaking. This method had a variety of difficulties due to the low time resolution in the data. The cross-correlator tried to match up the sinusoids, but the time delay was two to three data points so only a rough phase could be found. After hours of tweaking, the idea of hybridizing the two in some way began to take shape. After trying elegant and mathematically rigorous routines, it was the most rudimentary technique that provided what we sought. Although computationally inefficient, it allows the phase shift to be found at a degree of precision defined by the user, within the resolution of the data. Even when linear approximation does

not allow the theory to fit the data, a well defined velocity can be extracted. Only one data point has been extracted at the current time, but the algorithm will be used later on in the analysis.

This analysis has been beneficial in planning next data collection runs. Starting out we did not know what to look in the data to rate it as good or bad. Now knowing that we want data with a clear phase shift and has good temporal resolution. If the data does not fit this general description, the phase shift information will be hidden in the noise. Being able to analyze new data in almost real time will also help the data collection process, making sure the data being collected is providing the information being sought. In addition to providing a new data point on Fig. 7, we have developed a technique to focus the experimental process in the correct direction for acquiring more information about this new temperature-entropy wave.

References

[1] Bak, P. *How Nature Works*. (Copernicus, Springer-Verlag. New York, 1996).

[2] H. Baddar, G. Ahlers, K. Kuehn, and H. Fu. J. Low Temp. Phys. **119**, 1 (2000).

[3] R.V. Duncan, G. Ahlers, and V. Steinberg Phys. Rev. Lett. **60**, 1522 (1988).

[4] B.J. Klemme, M.J. Adriaans, P.K. Day, D.A. Sergatskov, T.L. Aselage, R.V. Duncan, J. Low Temp. Phys. **116** (1999).

[5] W. A. Moeur, *Thermal Conductivity Measurements in* ^{4}*He Near the Superfluid Transition Temperature*. Dissertation - *Univ. of New Mexico* (1997).

[6] W. A. Moeur, P. K. Day, F-C. Liu, S. T. P. Boyd, M. J. Adriaans, R. V. Duncan Phys. Rev. Lett. **78**, 2421 (1997).

[7] D. A. Sergatskov, A. V. Babkin, R. A. M. Lee, S. T. P. Boyd, R. V. Duncan Physica B. 329-333, **208** (2003).

[8] P.B. Weichman, J. Miller, J. Low Temp. Phys. **119** (2000).

[9] Phase Diagram - http://boojum.hut.fi/research/theory/helium.html

[10] W.Y. Tam and G. Ahlers, Phys. Rev B **32**, 5932 (1985; **33**, 183 (1986).

[11] R.A. Ferrell, N. Menyhard, H. Schmidt, F. Schwabl, P. Szepfalusy, Phys. Rev. Lett. 18 (1967) 891.

[12] M. Dingus, F. Zhong, and H. Meyer, J. Low Temp. Phys. **65**, 185 (1986).

Acknowledgments

I would like to thank Dr. Robert Duncan for being a great mentor and teacher. Paul Martin for working with me on the project, wading through the data and helping come up with new ideas while developing the code. I would also like to extend thanks to Q. Li, S.T.P. Boyd, D. Sergatskov, and S. Rodrigue for their help.